

Improving Power Line Detection Based on Phase Difference in Radar Image

Dianqi Li*, Haoming Chen†, Darren S. Goshi‡, Ming-Ting Sun*

* University of Washington, Seattle, WA 98105 USA

† Google, Inc., Kirkland, WA 98033 USA

‡ Honeywell Corporation, Torrance, CA 90504, USA

E-mail: {dianqili, mts}@uw.edu, haominghoward@gmail.com, Darren.Goshi@honeywell.com

Abstract—Previous framework on automatic power line detection based on millimeter-wave radar videos assumes the Bragg pattern of power lines are distinguishable with the background signals. This limits its ability in recognizing fine-grained power line signals within complex and noisy scenes. In this work, we propose a detection method that combines both characteristics of the amplitude and phase of the return radar signal. Experiments demonstrate that our proposed approach is able to detect the power lines accurately, efficiently and more robustly on a new two-channel dataset.

I. INTRODUCTION

High-voltage power lines present hazardous operating conditions for the helicopters especially when the pilots vision is degraded by obscurants such as dust, smoke, fog, rain, and snow [1], [2]. Radar can detect objects under poor visibility conditions, including at night. Unlike RGB cameras, a radar system is largely independent of the environment lighting condition. For example, while power lines are usually subtle in a video captured by an RGB camera, the metal surface structure of the power lines can make them much more visible in the radar signal. A few previous systems have been developed for power line detection with radar. In [3], a Passive Millimeter-Wave (PMMW) radar system is tested to image power lines from a vehicle. The power lines in the PMMW radar signal are reported to have higher contrast than in RGB images, but they are still not very visible. In [4], the Radar Cross-Section (RCS) model of power lines is developed, and the authors observe the Bragg-pattern which is a distinguishing feature of the power lines in the radar signal due to their periodic surface structure. A polarimetric detection algorithm is further proposed in [5] [6] by Sarabandi et al. for detecting power lines. However, this approach is primarily proposed for the Synthetic Aperture Radar (SAR), which is not especially suitable for helicopters that could fly at the same height as the towers and the power lines. Later, an automatic power line detection framework [7] [8] principally based on image processing and machine learning was proposed to solve this issue using the radar amplitude image.

In this paper, we propose to incorporate the phase difference information into the detection algorithm to improve the results under difficult situations. We collect a new two-channel radar dataset that represents more challenging conditions and show that we can achieve more robust results compared to the

⁰This work was done while Haoming Chen was a Ph.D. student at University of Washington.

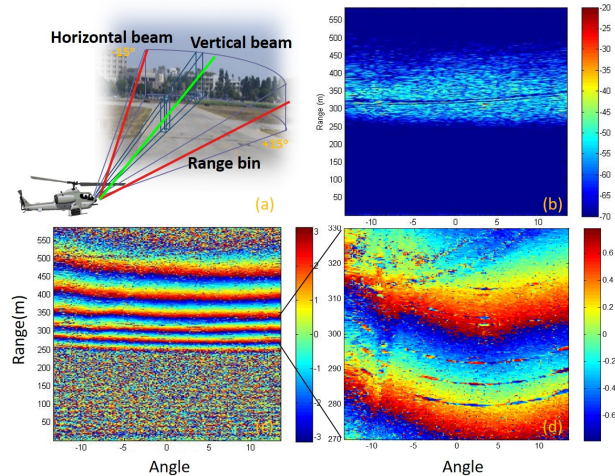


Fig. 1. (a) An illustration of our two-channel object detection system in a helicopter. (b). The amplitude image from the two-channel radar system. (c). The phase difference image from the two-channel radar system. (d). An enlarged phase region that includes power line signals.

previous power line detection algorithm [7] [8]. Figure 1 shows the amplitude and phase difference channel provided by the new two-channel radar dataset. As can be seen from the figure, with a very strong ground noise return, the real power line is invisible from the amplitude image and the previous algorithm usually fails. However, the phase difference image pattern is gradually changing with the distance of the object. Hence, the power lines cause a discontinuity pattern on the phase difference image since the distance discriminates the power lines from the background. Based on this observation, we propose an algorithm to detect the discontinuous part representing the power line in the phase difference image even if the scene is complex and noisy. Experimental results demonstrate the effectiveness of the proposed detection approach.

II. RELATED WORK

The previous detection framework [7] [8] shown in Figure 2 first applies image processing algorithms to reduce the noises, and identify the possible candidates. Then, the coordinate transform maps the thresholded image in the polar coordinate to the Cartesian coordinate, so that the power line is a straight line on the image. This process is followed by a Hough transform [9],

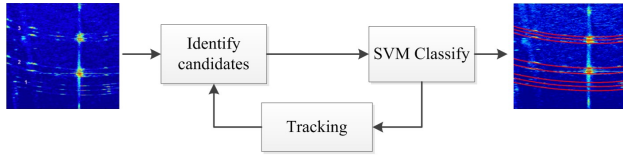


Fig. 2. Simplified diagram of existing detection algorithm [7] [8] (red lines in the output image show the locations of the detected power line)

which is a common approach for detecting straight lines in an image. It transforms the spatial domain image into the parameter domain. Each straight line can be represented in two parameters: ρ as the distance from a certain point (typically the origin) to the line, and θ as the orientation of the line. Thus, each straight line corresponds to a single point (ρ, θ) in the parameter domain.

The best candidates (ρ, θ) are chosen by the likelihood functions defined in [8]. This process is denoted as the identification step. Compared to the false power line, the true power line has a Bragg pattern on the amplitude image. Therefore, a pre-trained Support Vector Machine (SVM) classifier [10] is used to determine if each candidate is a real power line or a noise line. In the video sequence, the best (ρ, θ) candidate in each frame are tracked by a particle filter algorithm [11] that receives the feedback from the SVM classifier. More detailed formula and descriptions can refer to [7] [8].

III. POWER LINE DETECTION USING PHASE IMAGES

The previous framework in [7] [8] works well in the cases that the Bragg patterns are clear in the amplitude channel (Figure 3(a)). However, in some cases, the return amplitude signals of power lines are hidden in the strong background noise. It is very difficult to detect the power line from the radar amplitude image for these cases. In this situation, the previous algorithm [7] [8] has a bad performance as the Bragg pattern of power lines can be hardly detected.

To overcome this problem, the phase image (as in Figure 3(b)) which contains the distance information of the objects can be utilized to assist the detection. For example, the phase difference value of the flat ground is gradually changing as the distance keeps continuously changing. However, due to the power line and the background are located at different distance locations, the phase values on the power lines are not continuous with its background neighboring pixels, so a discontinuity pattern can be seen on the phase difference image. By using this phenomenon, the phase difference image can be used to detect the power line. Previous algorithm [7] [8] on the amplitude image cannot be directly applied on the phase difference image. To fully utilize our previously developed framework [7] [8], a method is to remove the continuous background phase pattern so that power line patterns can be strong signals compared to the rest regions. In the following parts, we discuss some details of extraction and detection of the power lines using the phase difference images.

1) *Separate the strong and weak noise regions:* Our previous framework on the amplitude image works well for weak noise

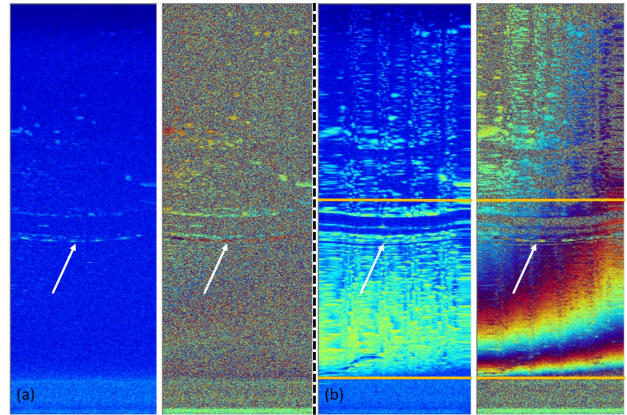


Fig. 3. Two cases in the amplitude (left) and phase difference (right) image: (a) Relatively weak noise amplitude with random phase difference. (b) Relatively strong noise amplitude with smoothly changing phase difference (white arrows point to the power lines). The orange boundaries denote the cropped active region. The colors represent different magnitudes.

regions, so it is natural that we can separate the image into strong noise and weak noise regions and apply the different algorithms. To locate the strong noise region, a simple cropping method is used to separate the image into two parts, an active part and an inactive part. The active part is the part where the average intensity is larger than a certain value. The cropped active region (Figure 3(b)) in the phase difference image is further processed by the unwrapping algorithm in the next step. Meanwhile, we apply an empirical threshold: 0.8, on the amplitude image to generate a noise mask N (1: amplitude > threshold, 0: otherwise). It is worthwhile to note that the same mask can also be used to remove the random noise in the phase difference image, which is beneficial to the later phase unwrapping process.

2) *2D phase unwrapping:* Applying the power line detection algorithm directly on the cropped region has two main problems. First, due to the nature of the phase values, the phase difference value is wrapped and not continuous at the boundary, where it has the jumping part from $-\pi$ to π (blue region to red region in Figure 3(b)). Hence, general background remove methods failed due to the 2π discontinuities, which may lead to false detections. Second, as mentioned above, the cropped region still contains plenty of noises. It is hard to track the tendency of the phase value with the discontinuities caused by the noises. To address the two issues, we follow [12] and [13] to unwrap and smooth the noisy phase difference image.

Different from the 1D phase unwrapping algorithm, the 2D phase unwrapping need to be path-independent. Goldstein et al. [12] point out that unwrap path dependency is caused by point-like sources called residues. A residue is the clockwise sum of wrapped phase differences around a loop of four neighboring pixels. By introducing the phase wrapping operator

$$W(\phi) = (\phi \bmod 2\pi) - \pi, \quad (1)$$

the $W(\phi)$ is constrained in the $(-\pi, \pi]$, where ϕ is the wrapped phase difference value, and n is a integer. Then, the residue map R can be calculated in counterclockwise direction around each

pixel by:

$$R_{i,j} = \frac{1}{2\pi} [W(\phi_{i+1,j+1} - \phi_{i+1,j}) + W(\phi_{i+1,j} - \phi_{i,j}) + W(\phi_{i,j} - \phi_{i,j+1}) + W(\phi_{i,j+1} - \phi_{i+1,j+1})], \quad (2)$$

where (i, j) is the location in the phase difference map, $R_{i,j}$ can have the value 0, -1, +1.

According to the theorem of loop integral [14], if all closed paths are constrained to enclose zero net residue, then the phase difference sum around any path is zero, and the unwrapped phase is defined uniquely. However, based on the obtained residue map, non-zero residues are not guaranteed in everywhere. Therefore, a constraint is imposed by forming the residues in clusters, each with zero residue sum, and requiring the unwrapping path enclose either all or none of the residues in each cluster. In the implementation, we cluster the nearby +1, -1 residues as well as the edges of the image (which can serve as a kind of arbitrary residue) to create a branch cut mask M whose sum residue is zero in everywhere. In this condition, any path made up entirely of unmasked pixels is guaranteed to be suitable for unwrapping.

$$\oint W(\nabla\phi) \cdot d\mathbf{r} \equiv 0. \quad (3)$$

Therefore, the original phase difference value can be obtained by the path integral along the unmasked path

$$\varphi(q) = \int_s^q W(\nabla\phi) \cdot d\mathbf{r} + \varphi(s), \quad (4)$$

where $W(\nabla\phi)$ denotes the phase derivative in the phase difference image after the wrapping operator. φ denotes the phase difference value after unwrapping. s is the starting point of the path integral. Note that the path from point s to point q should follow the unmasked regions.

Although the mask M suggests the forbidden region for unwrapping, there are still thousands of possible integral paths to choose. A path mixed with too many random noises will lead to an unfavorable unwrapping result. Choosing a correct path to unwrap the phase value is essential. Following [13], the unwrapping results can be simply guided by a quality map, which indicates the reliability of the measurements. In our implementation, we use the negative variance map from the phase image as the quality map Q :

$$Q_{m,n} = - \sum_d \frac{\sqrt{\sum_{i,j} (W(\nabla_d\phi_{i,j}) - \overline{W(\nabla_d\phi_{m,n})})^2}}{k^2}, \quad (5)$$

where the k is the kernel size to calculate the variance. (i, j) is the adjacent pixel index near the index (m, n) . d can be x or y , and $\overline{W(\nabla_d\phi_{m,n})}$ means the wrapped average phase derivative value along x or y axis in the kernel size range of index (m, n) .

With the quality map, the algorithm first unwraps the phase value of the pixel with the highest quality value along the path indicated by branch cut mask M and noise mask N . An intuitive idea is that non-noisy or continuous regions should have smoother phase difference values, indicating these regions should have lower variance and higher quality. Therefore, the

quality-guided phase unwrapping algorithm can accurately unwrap and restore the original phase difference without involving too many noisy pixels. After all unmasked pixels have been unwrapped, the masked pixels that adjoin unwrapped pixels are unwrapped.

3) *Background Removal*: After the phase unwrapping algorithm, the power line is the only discontinuous pattern on the background with the gradually changing pattern. On the unwrapped phase image, a median filter can be applied to remove the power lines pattern (which is treated as noise), so that the background is obtained. By subtracting the background with the unwrapped image, the power line pattern can be extracted. There are two concerns how to choose the median filters: (1) the filter should cover more background pixels than the power line pixels, so that the median value is from the background; (2) The filter should not cover the noise region N so that the median value can be close to the background. Moreover, the phase difference image has a height of more than $8K$, and the phase values change more slowly along the y direction. Therefore, in our experiment, a tall median filter with a typical size of $101(\text{height}) \times 21(\text{width})$ pixels is applied to smooth the regions adaptively with the help of the noise mask N .

4) *Adaptive Power Line Detection*: After extracting the power line pattern in the phase difference image, we can apply the identification step [7] to extract the line candidates from the parameter domain. As mentioned in the previous part, the phase difference image based power line detection is more beneficial for the strong noise region and the amplitude image based detection is more suitable for the weak noise region. So, a combination of these two methods is suitable to cover different cases. In our experiment, it is straightforward to process these two types of regions separately with different algorithms and then combine the detected results together. The quantitative results are shown in the experiment section.

IV. EXPERIMENTAL RESULTS

A. Dataset and Ground Truth Collection

We collect a new dataset containing more challenging situations for testing our proposed algorithm. The whole dataset consists of an old collection (magnitude image only) and a new collection (magnitude and the phase-difference images). The old collection and new collection have 617 frames and 204 frames in total, respectively. Compared to the old collection which contains only magnitude images, the new collection provides the amplitude image and the phase difference image for detecting power lines. Moreover, the new collection has more complicate and difficult scenes to detect power lines.

The SVM classifier is the core in the power line detection algorithm, thus, accurate labels for the training and testing are necessary. In the previous work [7] [8], the candidate lines are generated by the identification step and the corresponding labels are manually checked with the original video by the eyes. This process has two problems: (1) The identification step may miss parts of real power lines, leading to an incomplete training dataset; (2) If the algorithm is updated, we may need to

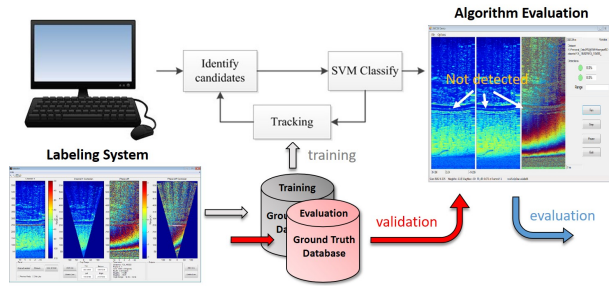


Fig. 4. An illustration of data labeling and auto evaluation framework.

TABLE I
DETECTION RESULTS COMPARISON BASED ON PREVIOUS DATA LABELING METHOD AND OUR NEW DATA LABELING METHOD. THE RESULTS ARE EVALUATED ON AMPLITUDE IMAGE ONLY USING ALGORITHM IN [7] [8]

Dataset	Old Labeling		New Labeling	
	Precision	Recall	Precision	Recall
Old collection	93.21%	88.83%	94.33%	90.08%
New collection	30.47%	54.25%	60.27%	72.17%

manually re-label all new lines, which is quite inefficient. Based on the above observations, we developed an efficient labeling system with the ground truth database that can be used for both algorithm training and evaluation.

The system is illustrated in Figure 4. In the system, all the power lines (ground truth) are accurately labeled with our labeling tool on the whole dataset in advance. The SVM training data can then be easily obtained from the ground truth dataset. To evaluate the detection performance of the algorithm, we built a real-time evaluator that displays the detection visualization as well as the evaluation metric. For each detected line with its orientation and distance, the nearest line in the ground truth dataset is selected. If the distance between the ground truth and the candidate is larger than 2 pixels, the detected line is regarded as a false detection.

By using the datasets we collected, we can label and access the ground truths in each frame. We randomly sample 700 real power lines and 1000 false power lines from the amplitude channel as the training set for the SVM classifier with Gaussian kernel. The rest of frames are used for detection testing.

B. Data Labeling Method

To validate the new data labeling method is superior than the old one, we first compare the detection results on the amplitude image with the training data from different methods. Following the evaluation protocol in [1], we calculate the precision and recall metrics on the whole dataset. As can be seen in Table I, the SVM model trained on the new data labeling framework can achieve a slightly better performance on the old collection, and 30% precision and 20% recall boosting on the new collection dataset. We found most of failure cases come from the new collection dataset. This could be attributed to that the old data labeling method fails to capture all real power lines with background noises, leading to an incomplete training dataset. During testing, when the scenes are complex and noisy, more

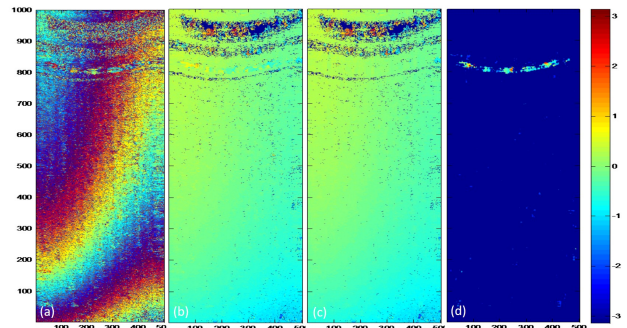


Fig. 5. Example of 2D phase unwrapping and background removal on real radar image. (a) The original phase difference image. (b) The unwrapping algorithm smooths the 2π discontinuities on the phase image. (c) The phase image after applying median filter with help of noise mask to exclude the power lines' signal. (d) Background removal method by subtracting (b) with (c).

real power lines are filtered by the identification step that is based on the Hough Transform. Additionally, the trained SVM model causes more false detection on the new collection dataset due to an incomplete training process. On the contrary, the new data labeling method accurately labels the real power lines in the whole sequences, even when the power line signals are mixed with dense background noises. Thus, the new SVM model largely reduces the false detection on each frame. This experiment reveals that a complete training dataset based on the new labeling method can improve the detection performance.

C. Phase Unwrapping and Background Removal

Although the new training data improve the detection performance, some frames in the new collection dataset still have uncommon false detection using the algorithm in [7] [8]. In these frames, the background is so noisy that the identification step cannot locate the true power lines. To relieve this situation, the phase difference image provided by the new collection dataset can assist the detection. Figure 5 shows the intermediate stages of the proposed phase unwrapping algorithm and background removal method. As can be seen, the proposed phase unwrapping algorithm effectively unwraps the phase values and smooths the 2π discontinuities in the phase background pattern. Since the discontinuities of the power line signals and other random noises do not share the same characteristics, those signals are kept after the unwrapping process. Note that the random noise region can be indicated by the noise mask N obtained through the previous region separation process. By ignoring the noise region, the power line signals can be easily extracted by the proposed background removal method. As a result, the processed phase difference image has relative clear background and can be utilized by our previous detection framework. The quantitative results demonstrate our proposed algorithm can effectively eliminate the background and noise signals in the phase difference channel, resulting in a suitable image for the following power line detection.

D. Detection with the Phase Difference Image

The phase unwrapping algorithm and background removal method contribute a clean image for power line detection. We

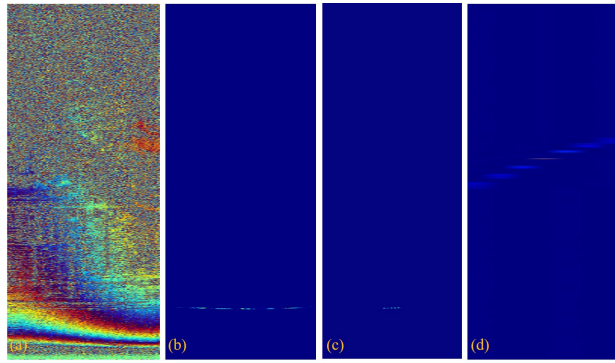


Fig. 6. Examples of line detection on phase difference image. (a) The original phase difference image. (b) The phase difference image after background removal method. Only the signals of power line are kept. (c) Coordinate transformation on (b). (d) Hough transformation on (c). The red point represents the parameters of the kept power line.

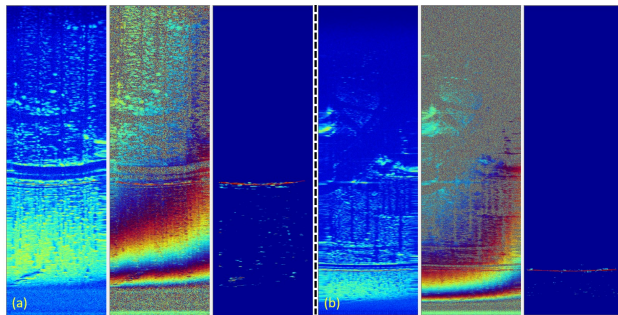


Fig. 7. Two detection examples by using phase difference image. In each side, from left to right: amplitude image, phase difference image and phase difference image after background removal. The red lines denote the detection results.

use our previous architecture [7] [8] to detect the power line in the phase difference image. Figure 6 shows that after the background removal, only the power line signals are kept. Without the interruption of noises, the algorithm correctly identifies the most likely location of power lines. As a result, the identification step can rapidly locate the real power lines even without much help from the SVM classifier. Some detection results are shown in Figure 7. We see that the power lines can be detected accurately from the phase difference image after the background removal method.

To this end, we compare the detection results from the previous approach [7] [8] and the results from the adaptive approach on the new collection dataset. Table II shows that our adaptive approach achieves a better performance when the background signals are noisy and covering the power lines. The result suggests that the proposed phase algorithm is capable of removing the background noises, and benefiting the detection cases that have difficulties using amplitude channel alone.

V. CONCLUSION

In this report, we propose an adaptive power line detection framework using image processing and machine learning to

TABLE II
DETECTION RESULTS ON THE NEW COLLECTION DATASET. AMPLITUDE MODEL ON DETECT THE POWER LINES IN AMPLITUDE IMAGE. THE ADAPTIVE MODEL COMBINES BOTH RESULTS ON AMPLITUDE AND PHASE DIFFERENCE IMAGES

Model	Precision	Recall
Amplitude Model	60.27%	72.17%
Adaptive Model	86.16%	89.12%

combine the characteristics from both amplitude and phase difference radar images. We investigate and improve our early effort on the power line detection framework. Based on the two-channel feature of the new dataset, we first proposed a phase difference based detection algorithm, which can help to detect the power line on a noisy background. We also develop the data labeling framework and testing platform for training the model and testing results that confirm the effectiveness of our method.

With a higher resolution radar video, and the extra phase difference image processing, the computation complexity is much higher. It is desirable that the algorithm can be implemented using parallel processing so that real-time detection can be achieved using a low-cost FPGA chip or GPU.

REFERENCES

- [1] J. S. Harris, "Data show 50 us-registered helicopters involved in wirestrike accidents from 1996 through 2000," *Flight Safety Quarterly*, Sep, no. 32, pp. 8–15, 2002.
- [2] Ö. E. Yetgin, Z. Şentürk, and Ö. N. Gerek, "A comparison of line detection methods for power line avoidance in aircrafts," in *Electrical and Electronics Engineering (ELECO)*. IEEE, 2015, pp. 241–245.
- [3] R. Appleby, P. Coward, and J. N. Sanders-Reed, "Evaluation of a passive millimeter wave (pmmw) imager for wire detection in degraded visual conditions," in *Proc. SPIE*, vol. 7309, 2009, p. 7309A1.
- [4] K. Sarabandi and M. Park, "A radar cross-section model for power lines at millimeter-wave frequencies," *IEEE Transactions on Antennas and Propagation*, vol. 51, no. 9, pp. 2353–2360, 2003.
- [5] K. Sarabandi, L. Pierce, Y. Oh, and F. T. Ulaby, "Power lines: Radar measurements and detection algorithm for polarimetric sar images," *IEEE TAES*, vol. 30, no. 2, pp. 632–643, 1994.
- [6] M.-S. Park, "Millimeter-wave polarimetric radar sensor for detection of power lines in strong clutter background." Ph.D. dissertation, 2004.
- [7] Q. Ma, D. S. Goshi, Y.-C. Shih, and M.-T. Sun, "An algorithm for power line detection and warning based on a millimeter-wave radar video," *IEEE TIP*, vol. 20, no. 12, pp. 3534–3543, 2011.
- [8] Q. Ma, D. S. Goshi, L. Bui, and M.-T. Sun, "Robust power line detection with particle-filter-based tracking in radar video," *APSIPA Transactions on Signal and Information Processing*, vol. 4, 2015.
- [9] L. Shapiro and G. C. Stockman, "Computer vision. 2001," ed: Prentice Hall, 2001.
- [10] C. Cortes and V. Vapnik, "Support vector machine," *Machine learning*, vol. 20, no. 3, pp. 273–297, 1995.
- [11] P. Del Moral, "Non-linear filtering: interacting particle resolution," *Markov processes and related fields*, vol. 2, no. 4, pp. 555–581, 1996.
- [12] R. M. Goldstein, H. A. Zebker, and C. L. Werner, "Satellite radar interferometry: Two-dimensional phase unwrapping," *Radio science*, vol. 23, no. 4, pp. 713–720, 1988.
- [13] T. J. Flynn, "Consistent 2-d phase unwrapping guided by a quality map," in *Geoscience and Remote Sensing Symposium*, vol. 4. IEEE, 1996, pp. 2057–2059.
- [14] J. R. Rice *et al.*, "A path independent integral and the approximate analysis of strain concentration by notches and cracks." ASME, 1968.